Structural characterization of thin film photonic crystals

G. Subramania,[1] R. Biswas,[1] K. Constant,[2] M. M. Sigalas,[1] and K. M. Ho[1]
[1]*Department of Physics and Astronomy, Ames Laboratory and Microelectronics Research Center, Iowa State University, Ames, Iowa 50011*
[2]*Department of Materials Science and Engineering, Iowa State University, Ames, Iowa 50011*
(Received 15 November 2000; published 23 May 2001)

We quantitatively analyze the structure of thin film inverse-opal photonic crystals composed of ordered arrays of air pores in a background of titania. Ordering of the sphere template and introduction of the titania background were performed simultaneously in the thin film photonic crystals. Nondestructive optical measurements of backfilling with high refractive index liquids, angle-resolved reflectivity, and optical spectroscopy were combined with band-structure calculations. The analysis reveals a thin film photonic crystal structure with a very high filling fraction (92–94 %) of air and a substantial compression along the *c* axis (~22–25 %).

DOI: 10.1103/PhysRevB.63.235111 PACS number(s): 78.20.−e, 42.70.Qs, 82.70.Dd, 83.80.Hj

I. INTRODUCTION

Over the last few years a class of artificially engineered structures—photonic band-gap materials—have offered ''yet another'' way of light manipulation. Such materials possess periodic alternating regions of high and low indices of refraction in two or three dimensions and are characterized by a frequency gap where electromagnetic wave propagation is forbidden.[1–3] The wavelength of the gap is on the same length scale as the spatial modulation of the refractive index, making it a considerable challenge to synthesize such materials for visible and near-infrared frequencies.

Recently there has been a tremendous increase in the experimental fabrication of photonic crystals composed of a wide variety of materials and possessing interesting structural morphologies.[4–13] When these structures are probed for optical properties, various assumptions are made regarding the structural details which are based on the synthesis technique. In certain experimental approaches, drastic structural changes can occur during the intermediate processing steps, which may involve etching or heat treatment. These structural changes also offer a new way to tune the photonic properties. In this paper we have proposed simple, nondestructive techniques for probing the structural information of photonic crystals which can, in principle, be applied to samples irrespective of the processing technique used to fabricate the samples. We demonstrate this technique on thin-film inverse-opal photonic crystals synthesized by colloidal self-organization to estimate the fill fraction of air, *c*-axis compression, and an index of background material by comparing experimental data with band-structure calculations.

Understanding the optical behavior of naturally occurring opals[14] and their composition has paved the way for making photonic crystals at visible wavelengths. Monodisperse submicrometer-size spheres of silica and polystyrene are readily available in colloidal form and under suitable conditions can self-organize to form colloidal crystals of the fcc type. However, in order to obtain a full three-dimensional photonic frequency gap, theoretical models[15–20] favor the ''inverse'' fcc structure, which is air in place of the spheres in a background of high index dielectric.[15–18] Theoretical models[18,21] also indicate stringent requirements for a full gap, such as an index contrast higher than 2.9 and a minimal disruption of crystalline order. This has resulted in a wide variety of different innovative approaches to making visible frequency photonic crystals based on the colloidal crystal templates. Index contrast is sought using a wide choice of background materials: polymers, metals, ceramic precursors, oxide nanoparticles, and semiconductors.

Controlled crystal-growth techniques have been developed by various groups[4–9,11–13] to deal with the problem of disorder and other crystal defects. Depending on the approach the intermediate processing steps may introduce changes in the final structure obtained. For example, shrinkage of the lattice structure when using sol-gel precursors or oxidation of metal infiltrates can introduce certain structural distortions leading to deviations in measured optical properties from that obtained from simulation. Simple nondestructive spectroscopic measurements on the fully processed samples gives us extremely relevant structural information.

In this paper we determine the structure of our thin film photonic crystals from optical spectroscopy methods. In contrast to several recent growth approaches, we perform the ordering of the polystyrene spheres (that act as a template) and introduce the background titania simultaneously. The advantage of our technique over sol-gel approaches is that very large area films can be economically fabricated on any desired substrate, a highly desirable feature for infrared and optical coatings. Our results indicate a structure considerably distorted from the ideal photonic crystal structure. Theoretical simulations for the determined structure agree very well with the experimental measurements.

In this paper we investigate inverse-opal photonic crystals which have stop bands ranging from the optical (500 nm) to the near infrared (1100 nm). These photonic crystals have stop bands of width ~10–15 %. The widest stop band appears in the stacking direction.

II. SAMPLE PREPARATION AND FEATURES

The thin film samples are grown on glass substrates from a suspension that is a stabilized colloidal mixture of monodisperse polystyrene microspheres and nanocrystalline titania. Briefly, a colloidal suspension of polystyrene micro-

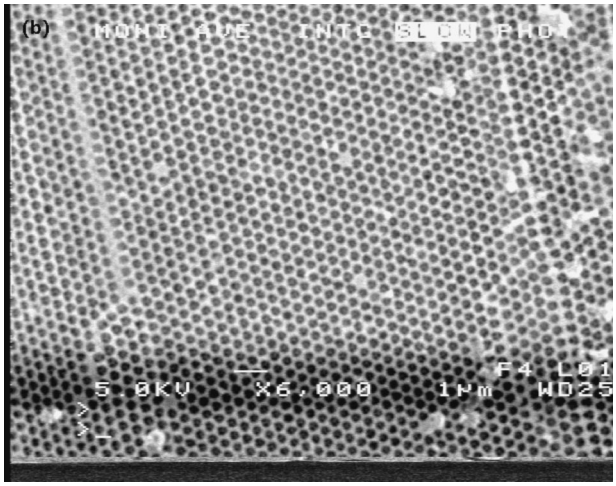

FIG. 1. Scanning electron microscope (SEM) image of an ordered domain of a thin film photonic crystal fabricated from 400-nm spheres.

spheres and nanocrystalline titania is prepared. The mixture is sonicated to break up agglomerates and spontaneous agglomoration is prevented by keeping the pH (8.6) above the isoelectric point of both types of particles. A few drops of this suspension is spread on a glass or silicon substrate and dried slowly in a humidity chamber at room temperature, over a period of about one day at a relative humidity of 90–95 %. During the drying process there is a spontaneous ordering of the polystyrene microspheres in the background of titania. The ordered regions appear as a strip in the upper region of the film, which shows a characteristic color.

The polystyrene spheres are then removed by heat treatment to 550 °C. The spheres are burnt out and the titania network densifies, resulting in air pores remaining behind in a titania matrix. Further details of the procedure are described previously.[22] The unique feature is the simultaneous formation of the ordered template of spheres and the synthesis of the titania background. Scanning electron microscopy (SEM) images[23,10] (Fig. 1) indicate that the crystal is stacked along the [111] direction and provide an accurate value of the in-plane lattice constant. Samples made with different sphere diameters show reflectivity peaks at differing wavelengths.[10] The peaks are due to the pseudogap, i.e., the lower depletion in the photonic densities of states, and match the reflected color seen with the naked eye in cases of smaller lattice constants.[23]

The peak wavelengths (Fig. 2) scale very well with the size of the spheres, indicating it is an intrinsic signature of the photonic stop band in the stacking direction. However, the measured peak wavelengths (Fig. 2) do not match those predicted from theoretical models under the assumption of a perfect fcc lattice of air spheres in a dielectric background. The measured wavelengths are 25–30 % smaller than that calculated for the ideal fcc photonic lattice. The experimental data correspond to $\lambda \sim 1.4D$, whereas $\lambda \sim 2.0D$ is theoretically expected for a close-packed array of air spheres, of diameter D, in a dielectric background of titania. The discrepancy is too large to be attributed to crystal quality. Further, the peak positions of the pseudogap are relatively in-

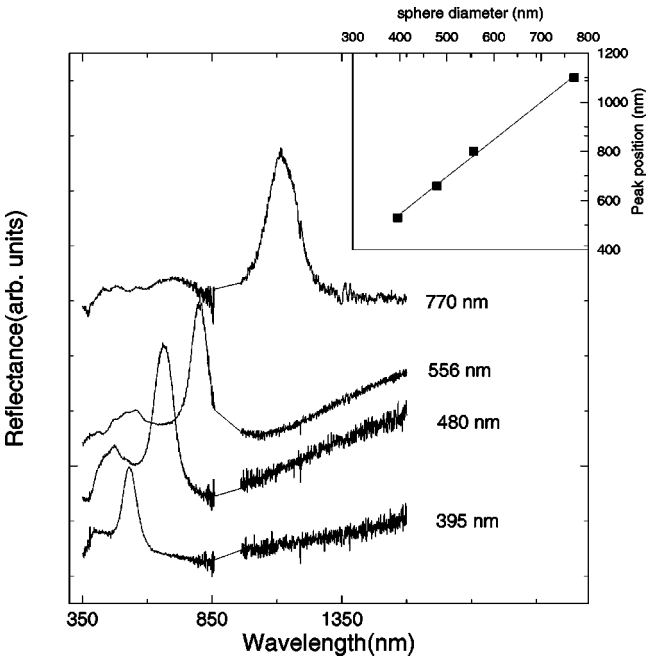

FIG. 2. Measured wavelength of the reflectivity peak as a function of the diameter of the air pores in the thin film colloidal crystal.

sensitive to stacking order and quite robust to disorder,[18,21] so that stacking disorder cannot account for the discrepancy in peak positions.

One possible source for the mismatch between theory and experiment can be seen from the shift in the peak position for the samples that undergo isostatic pressing to those without isostatic pressing (Fig. 3), which might suggest that the out-of-plane lattice constant is nonideal. Isostatic pressing was used to promote adhesion and to improve sample green strength before firing, since samples fired without pressing often tend to break apart. By synthesizing samples on substrates treated with appropriate surfactants this requirement may be eliminated. In addition to the isostatic pressing, during the firing stage other effects such as thin-film sintering,[24] as well as the sintering behavior of nanoparticles, can leave certain structural information unknown.

The gap position and optical properties depend on the following parameters whose exact values may have to be determined after the sample processing is complete: (i) the in-plane lattice constant, (ii) the out-of-plane lattice constant or the interplanar spacing d_{111}, (iii) the stacking sequence fcc (ABC) or hcp (ABAB) or a more complex sequence, (iv) the filling fraction of the air spheres, (v) the effective index of the background titania which is related to the porosity of titania matrix, and (vi) the shape of the air pores.

In Sec. III we describe two nondestructive spectroscopic measurements: optical measurements after back-filling the structure, and variable angle specular reflectance measurements, which are used to completely obtain the filling fraction, interplanar spacing, and the index of the background material. The in-plane lattice constant is directly obtained from the SEM images. Typically, there is a shrinkage of $\sim 5\%$ in the in-plane lattice spacing.

A lower limit on the index of the background titania was

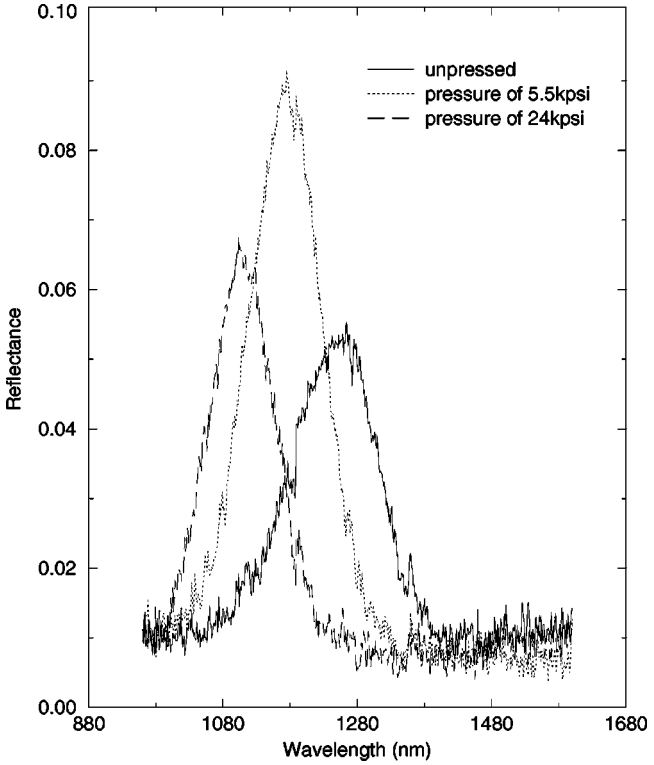

FIG. 3. Change in the reflectivity peak before and after the isostatic pressing to presuures of 5.5 and 24 kpsi. Data are for the 400-nm sphere sample.

immediately obtained by infiltrating the crystals with liquids up to index values of 1.9. The structure was still visible, indicating that the index of the background was indeed higher than 1.9. Liquids of higher index values were very viscous and dried too quickly to infiltrate the pores of the photonic crystal, making it difficult to perform index matching. So a partial index-matching technique was resorted to in which low refractive index liquids are infiltrated to measure the reflectivity peak shift. We compare the experimental data obtained with values obtained from simulations and extract structural information.

III. REFLECTANCE DATA OF INFILTRATED PHOTONIC CRYSTALS

Near-normal-incidence reflectance measurements probe the band structure along the ΓL direction [111] of the fcc structure. The frequency ν_L along the the stacking direction is given by

$$\nu_L = \frac{c_0}{n_{\text{eff}}}\frac{k_L}{2\pi} = \left(\frac{c_0}{n_{\text{eff}}}\right)\left(\frac{1}{d_{111}}\right)\left(\frac{1}{2}\right), \tag{1}$$

where c_0 is the speed of light and k_L is the wave vector at the L point. The effective refractive index of the crystal $n_{\text{eff}} = n_{\text{eff}}(f, n_2, n_1)$ as defined by Eq. (1) is a nonlinear function of the filling fraction f, the refractive index of the high index region n_2, and the refractive index of the low index region n_1, but is shown by the photonic band calculation to be insensitive to d_{111} for the structure studied here. Varying the refractive index n_1 by backfilling the air cavities, varies n_{eff}, and shifts the gap frequency (reflectance peaks) according to Eq. (1). Experimentally, this can be accomplished by infiltrating the crystals with liquids of different refractive indices. Samples were infiltrated with calibrated refractive index liquids with index values ranging from 1.3 to 1.39 obtained from Cargille Inc. Near-normal-specular-reflectance measurements were performed on samples made with 400-nm sphere templates using a Perkin Elmer Lambda-9 spectrophotometer and the shift in the peak position was plotted as a function of the index of the liquid infiltrated (Fig. 4). A wide sample surface area (6×1 mm^2) encompassing several grains was illuminated by the probe beam. The index liquids used for these measurements are free flowing and are readily drawn into the porous network of the photonic crystal by capillary action.

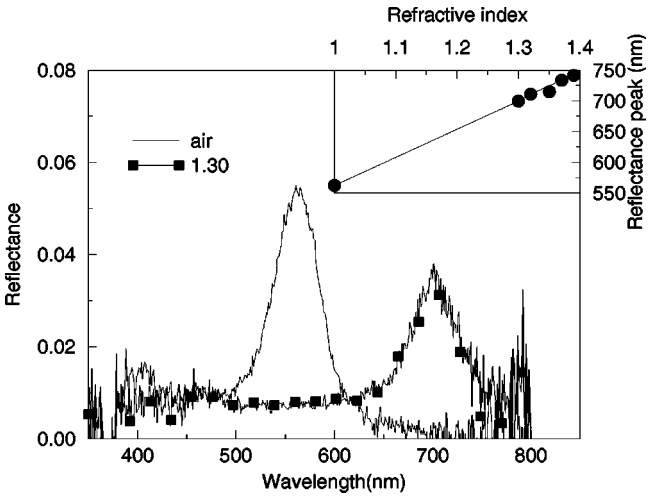

FIG. 4. Reflectivity peak before and after backfilling the photonic crystal with a liquid of refractive index 1.3. The inset shows the measured shift of the wavelength of the reflectivity peak as a function of the refractive index of the liquid.

In order to determine the range of the filling fraction we first consider the ratio of the L-point wavelengths, thereby eliminating the interplanar spacing (d_{111}) from Eq. (1),

$$\frac{\lambda_{liq}}{\lambda_{air}} = \frac{n_{\text{eff}}(f, n_2, n_{liq})}{n_{\text{eff}}(f, n_2, 1)}. \tag{2}$$

The L-point gap frequency is computed from photonic band-structure calculations as a function of the filling fraction by first assuming a refractive index of 2.7 for the titania network (n_2). The computation is repeated for the case when liquid with an index 1.3 is infiltrated (Fig. 5) and the ratio of the wavelengths for these two cases is plotted (Fig. 6) as a function of the filling fraction, as in Eq. (2). Since the compression of the structure is not determined at this stage of the analysis, we develop a self-consistent method to determine the compression. We start by assuming a compression in the structure [γ(guess)]. We calculate this ratio of wavelengths (2) for several guess compressions ranging from the ideal fcc structure to a structure with 30% compression [Fig. 6(a)]. The experimentally measured wavelength ratio (2) is found

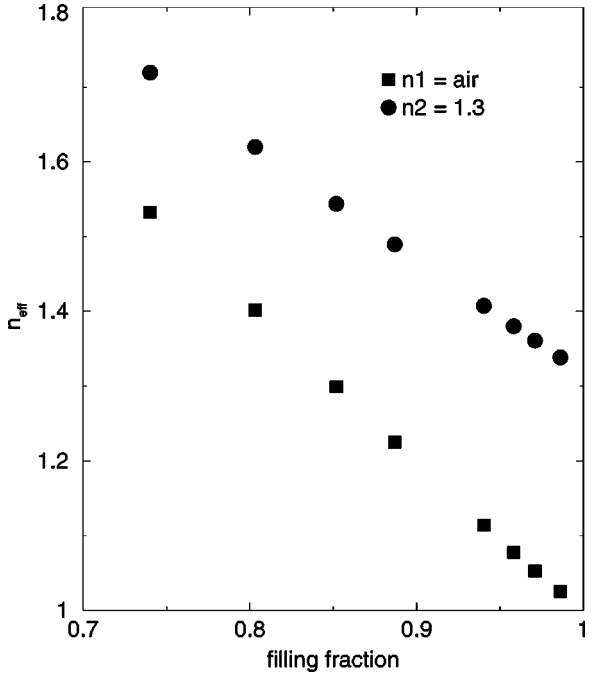

FIG. 5. The effective refractive index n_{eff} calculated from the photonic band structure (points). In the upper plot (squares), the pores are filled with a liquid of refractive index 1.3.

to be 1.245. The place where this experimental ratio intersects the theoretical curves, for the different guess compressions [Fig. 6(a)], yields a narrow range of filling fractions between 0.92–0.94. This indicates that this analysis and the use of wavelength ratios separates the compression from the other structural variables.

For each of the assumed compressions, and corresponding filling ratios, we use band-structure calculations to find the L-point frequency ν_L, which then determines the effective refractive index from

$$n_{\text{eff}}=\frac{c_0}{a}\frac{\sqrt{3}}{2}\frac{1}{\nu_L\gamma}. \tag{3}$$

Here a is the in-plane lattice constant. We use this n_{eff} value and the experimentally measured peak wavelength (λ_L) to determine the interplanar spacing d_{111} and hence the calculated output compression along the c axis γ(calc), using the following relations:

$$\lambda_L=2n_{\text{eff}}d_{111}, \tag{4}$$

$$\gamma=\frac{d_{111}}{\sqrt{\frac{2}{3}}D}. \tag{5}$$

We plot the output compression as a function of the input compression γ(guess) [Fig. 6(b)]. The self-consistent solution is when the input and output compressions match and this occurs for a substantial compression of 0.77–0.78 (i.e., 22–23 %). It is worth noting that the calculated compression lies in a narrow band between 21–24 % for all the inputed

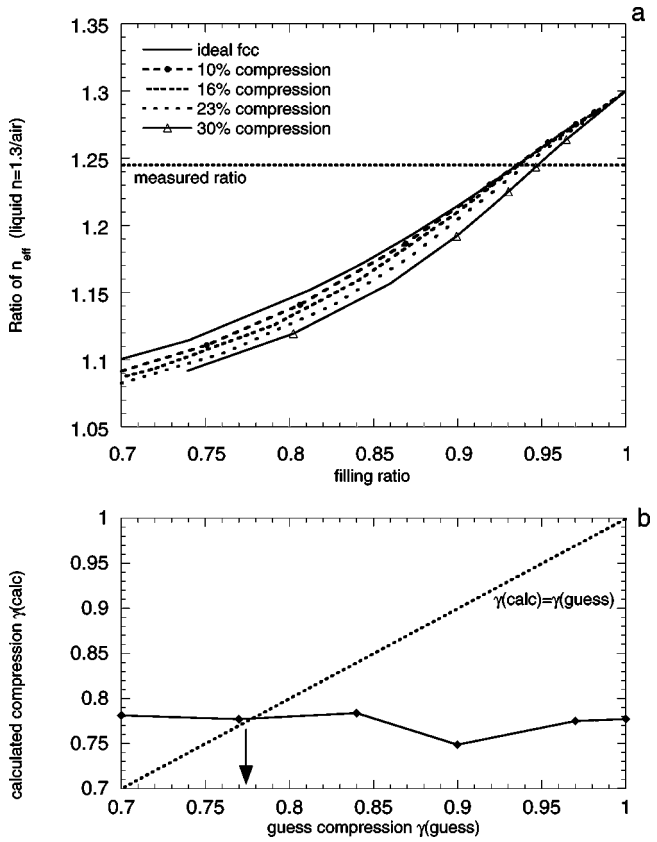

FIG. 6. (a) The ratio of effective refractive indices when pores are filled with liquid relative to the air-filled pores. Different curves correspond to the different values of the compressions used in these calculations. The dotted line shows the experimentally measured ratio. (b) The calculated compression (which is the output of the analysis) is plotted as a function of the input guess compression used in the analysis. The self-consistent solution is found when the calculated and guess compressions are the same, and is indicated by the arrow.

guess values [Fig. 6(b)]. We estimate the error in compression to be approximately 1%, arising from numerical analysis.

We recompute the wavelengths from the photonic band approach for different backfilling liquids with the values obtained for a filling fraction and compression and the value $n_2=2.7$. The values are consistent with the peak shift obtained for other index liquids (Fig. 7). The determined structural parameters provide an excellent fit to the reflectivity peak wavelengths for the different sphere diameters. The fit to the optical data is insensitive to the stacking: both fcc as well as hcp yield the same results. The fits to the data can be obtained for the range $n_2\sim 2.5-2.7$. Lowering the value of n_2 further reduces the compression and is not consistent with the optical data for $n_2<2.4$. At the optical wavelengths near green, the theoretical value for the index can even reach 3.0. The photonic crystal samples treated to higher temperatures (700 °C–800 °C) do not show significant change in the reflectance peak position. This would indicate that the background titania might be highly densified and so n_2 can be closer to the upper limit of 2.7.

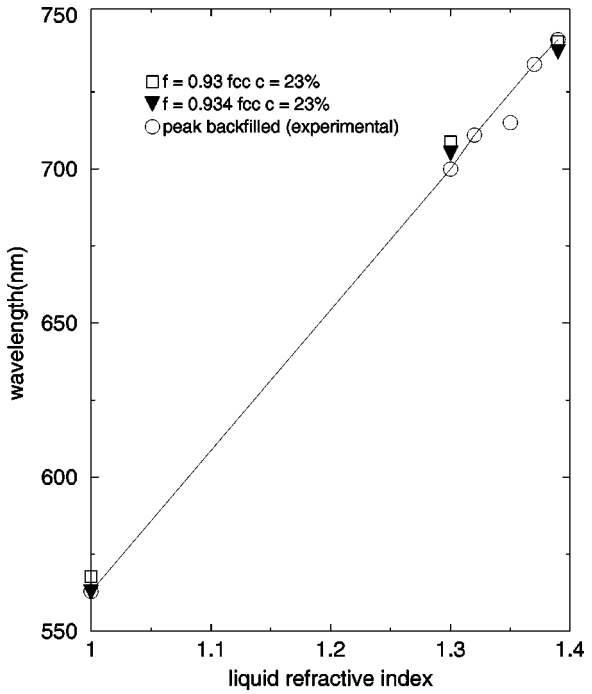

FIG. 7. Measured wavelengths of the optical reflectivity peak after backfilling the pores with liquid (circles). The straight line is a fit to the measurement. The calculated values of the reflectivity peak for an air-filling ratio of 93% and a compression of 23% are shown by the filled squares and triangles.

IV. BRAGG DIFFRACTION FROM PHOTONIC CRYSTAL

We measure the specular reflectance spectrum from the photonic crystals as a function of the incident angle. The peak shifts towards blue as the incident angle tilts away from the normal (Fig. 8), as seen in other inverse-opal photonic crystals.[11,25] This first-order Bragg diffraction contains the information about the interplanar spacing. If we assume that the system can be represented by a stack of uniform dielectric slabs with a refractive index of n_{eff} and thickness d_{111} then a simple analysis can be performed. Then the Bragg diffraction relation describing this effect is given by

$$2d_{111}(n_{\text{eff}}^2-\cos^2\phi)^{1/2}=m\lambda. \tag{6}$$

Here d_{111} is the interplanar spacing, n_{eff} is the effective refractive index of the composite medium, and ϕ is the angle of the incident beam with the surface. For first-order diffraction ($m=1$) a plot of λ^2 against $\cos^2\phi$ yields a straight line[11] with a slope $4d^2$ and intercept $4d^2n_{\text{eff}}$. The experimentally obtained data points fit this plot very well confirming the validity of the diffraction theory of our photonic crystal (Fig. 9) and the analysis of infiltrated inverse opals.

From the slopes of the plots one can directly obtain the interplanar spacing (Fig. 10), independent of the analysis in Sec. III. The compression along the [111] axis is $\gamma=d/[(\frac{2}{3})^{1/2}D]$ [Eq. (4)], where D is the diameter of the air

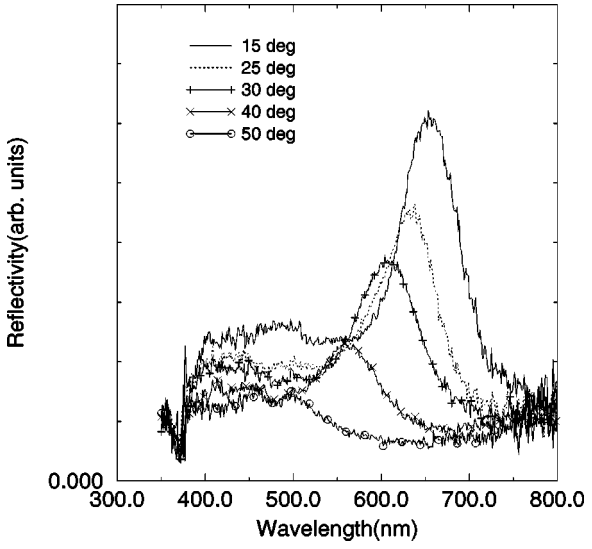

FIG. 8. Measured wavelength of the optical reflectivity peak as the incident beam is shifted away from the normal by 15° to 45°. These data were taken with the photonic crystal fabricated from 480-nm spheres.

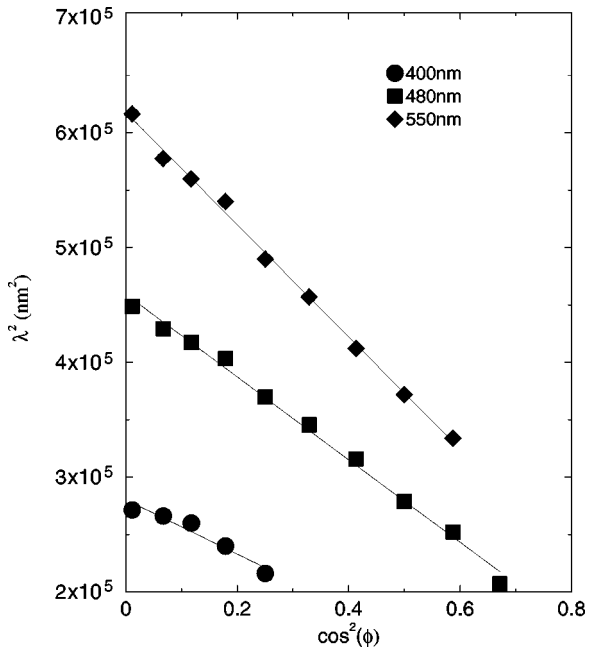

FIG. 9. Square of the wavelength of the reflectivity peak as a function of $\cos^2\phi$, where ϕ is the angle of the incident beam with the surface. The slope of the curve is $2d_{111}$.

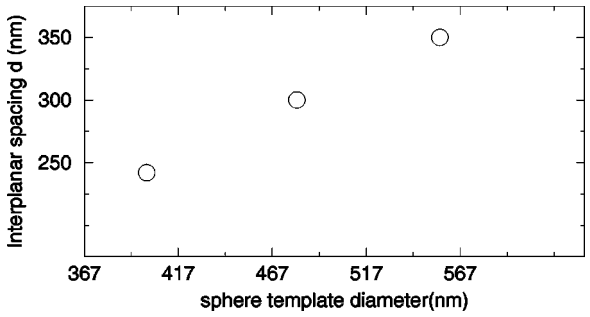

FIG. 10. Interplanar spacings extracted from the slopes of Fig. 9 for the different size photonic crystals.

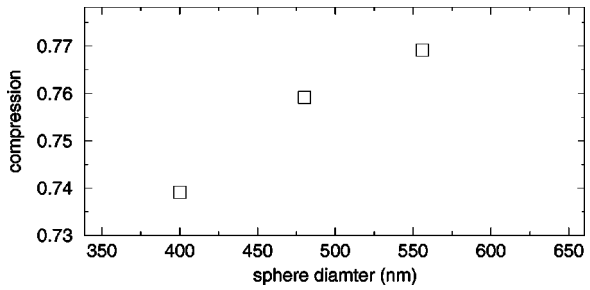

FIG. 11. The compression along the *c* axis extracted from the angle-resolved reflectance data (Fig. 9) as a function of the sphere diameter.

pores in the lateral direction measured from the SEM. Measuring the slopes and intercepts for photonic crystals synthesized from different diameter spheres (see Fig. 11), we obtained interplanar spacings that were contracted by 22–25 % from the ideal value. This value of the contraction independently confirms the analysis of the infiltration experiments of the preceding section. A slightly greater variation in compression (2%) is found in the diffraction data, probably because we are probing the compression for different photonic crystals with varying pore diameter. The results of both Secs. III and IV suggest compressions in the range of 22–25 %, allowing for both variation with pore size and in the numerical analysis.

The effective index n_{eff} falls in the range of 1.09 to 1.15. Such low values of n_{eff} arise from a large fraction of air in these photonic crystals.

V. RESULTS AND DISCUSSION

We have shown that simple nondestructive techniques can be used to characterize photonic crystals and obtain structural information such as interplanar spacing, and fill fraction of air/dielectric. First, the technique of specular reflectance measurements from the off-normal incidence angle is quite powerful yet very simple and gives us an independent way to obtain the n_{eff} and interplanar spacing. Knowledge of the interplanar spacing is quite crucial for comparing with any experimental data such as the measurement of spontaneous-emission suppression.

By infiltrating the photonic crystals with refractive index liquids with index values in the range of 1.3–1.4 we change the n_{eff} of the composite photonic crystal medium which shifts the reflectance peaks corresponding to the *L* point to a higher wavelength. By combining band-structure computations with the measurements, we uniquely determined values of n_{eff} and compression that agree very well with those obtained from variable angle spectroscopy. We obtain a filling fraction of air to be in the range of 92–94 %. For the thin film photonic crystals synthesized here we obtain an interplanar spacing that is 22–25 % smaller than the expected value for close-packed stacking. The entire set of optical data is fit very well by calculations for this structural geometry.

The shift of the reflectivity peak on isostatic compression offers a way to generate tunable photonic crystals from colloids by varying the isostatic pressure. The compression of the interlayers of our photonic crystal are analogous to the well-known interlayer reconstructions known for semiconductor and metal surface. In summary, we have demonstrated here a technique for characterizing photonic crystals and uniquely determining the structure of the photonic crystals.

ACKNOWLEDGMENTS

We acknowledge Costas Soukoulis for many helpful suggestions and discussions. Ames Laboratory is operated by the U.S. Department of Energy by Iowa State University under Contract No. W-7405-Eng-82. We also acknowledge support by the Department of Commerce through the Center for Advanced Technology Development (CATD) at Iowa State University.

[1] E. Yablonovitch, Phys. Rev. Lett. **58**, 2059 (1987).
[2] S. John, Phys. Rev. Lett. **58**, 2486 (1987).
[3] K.M. Ho, C.T. Chan, and C.M. Soukoulis, Phys. Rev. Lett. **65**, 3152 (1990).
[4] A. Zakhidov, R.H. Baughman, Z. Iqbal, C. Cui, I. Khayrullin, S. O. Dantas, J. Marti, and V.G. Ralchenko, Science **282**, 897 (1998).
[5] B.T. Holland, C.F. Blanford, and A. Stein, Science **281**, 538 (1998).
[6] A. Imhof and D.J. Pine, Nature (London) **389**, 948 (1997).
[7] G. Subramanian, Vinothan N. Manoharan, James D. Thorne, and David J. Pine, Adv. Mater. **11**, 1261 (1999).
[8] J.E.G. Wijnhoven and W.L. Vos, Science **281**, 802 (1998).
[9] A. Velev, T.A. Jede, R.F. Lobo, and A.M. Lenhoff, Nature (London) **389**, 448 (1997).
[10] G. Subramania, K. Constant, R. Biswas, M. Sigalas, and K.-M. Ho, Appl. Phys. Lett. **74**, 3933 (1999).
[11] A. Richel, N.P. Johnson, and D.W. McComb, Appl. Phys. Lett. **76**, 1816 (2000).
[12] S.G. Romanov, A.V. Fokin, H.M. Yates, M.E. Pemble, N.P. Johnson, and R.M. De La Rue, IEE Proc.: Optoelectron. **147**, 138 (2000).
[13] A. Blanco, E. Chomski, S. Grabtchak, M. Ibisate, S. John, S. W. Leonard, C. Lopez, F. Meseguer, H. Miguez, J.P. Mondia, G.A. Ozin, O. Toader, and H.M. van Driel, Nature (London) **405**, 437 (2000).
[14] J.V. Sanders, Acta Crystallogr., Sect. A: Cryst. Phys., Diffr., Theor. Gen. Crystallogr. **24**, 427 (1968).
[15] H.S. Sözüer, J.W. Haus, and R. Inguva, Phys. Rev. B **45**, 13 962 (1992).
[16] Toshio Suzuki, K. Paul, and L. Yu, J. Opt. Soc. Am. B **12**, 570 (1995).
[17] Kurt Busch and Sajeev John, Phys. Rev. E **58**, 3896 (1998).
[18] R. Biswas, M. Sigalas, G. Subramania, and K.-M. Ho, Phys. Rev. B **57**, 3701 (1998).
[19] K.M. Leung and Y.F. Liu, Phys. Rev. Lett. **65**, 2646 (1990).
[20] Ze Zhang and Sashi Satpathy, Phys. Rev. Lett. **65**, 2650 (1990).

[21] R. Biswas *et al.*, Phys. Rev. B **61**, 4549 (2000).
[22] G. Subramania, K. Constant, R. Biswas, M. Sigalas, and K.-M. Ho, Synth. Met. **116**, 445 (2001).
[23] G. Subramania, K. Constant, R. Biswas, M. Sigalas, and K.-M. Ho, J. Lightwave Technol. **17 (11)**, 1970 (1999).
[24] M.N. Rahaman, *Ceramic Processing and Sintering* (Marcel Dekker, New York, 1995).
[25] M.S. Thijssen, R. Sprik, J.E.G. Wijnhoven, M. Megens, T. Narayanan, A. Lagendijk, and W.L. Vos, Phys. Rev. Lett. **83**, 2730 (1999).